

Apolipoprotein E4 genotype compromises brain exosome production

Katherine Y. Peng,^{1,2} Rocío Pérez-González,² Melissa J. Alldred,^{2,3} Chris N. Goulbourne,² Jose Morales-Corraliza,^{2,3} Mariko Saito,^{3,4} Mitsuo Saito,^{3,5} Stephen D. Ginsberg,^{2,3,6,7} Paul M. Mathews^{2,3,6,*} and Efrat Levy^{2,3,6,8,*}

*These authors contributed equally to this work.

In addition to being the greatest genetic risk factor for Alzheimer's disease, expression of the $\epsilon 4$ allele of apolipoprotein E can lead to cognitive decline during ageing that is independent of Alzheimer's amyloid- β and tau pathology. In human post-mortem tissue and mouse models humanized for apolipoprotein E, we examined the impact of apolipoprotein E4 expression on brain exosomes, vesicles that are produced within and secreted from late-endocytic multivesicular bodies. Compared to humans or mice homozygous for the risk-neutral $\epsilon 3$ allele we show that the $\epsilon 4$ allele, whether homozygous or heterozygous with an $\epsilon 3$ allele, drives lower exosome levels in the brain extracellular space. In mice, we show that the apolipoprotein E4-driven change in brain exosome levels is age-dependent: while not present at age 6 months, it is detectable at 12 months of age. Expression levels of the exosome pathway regulators tumor susceptibility gene 101 (TSG101) and Ras-related protein Rab35 (RAB35) were found to be reduced in the brain at the protein and mRNA levels, arguing that apolipoprotein E4 genotype leads to a downregulation of exosome biosynthesis and release. Compromised exosome production is likely to have adverse effects, including diminishing a cell's ability to eliminate materials from the endosomal-lysosomal system. This reduction in brain exosome levels in 12-month-old apolipoprotein E4 mice occurs earlier than our previously reported brain endosomal pathway changes, arguing that an apolipoprotein E4-driven failure in exosome production plays a primary role in endosomal and lysosomal deficits that occur in apolipoprotein E4 mouse and human brains. Disruption of these interdependent endosomal-exosomal-lysosomal systems in apolipoprotein E4-expressing individuals may contribute to amyloidogenic amyloid- β precursor protein processing, compromise trophic signalling and synaptic function, and interfere with a neuron's ability to degrade material, all of which are events that lead to neuronal vulnerability and higher risk of Alzheimer's disease development. Together, these data suggest that exosome pathway dysfunction is a previously unappreciated component of the brain pathologies that occur as a result of apolipoprotein E4 expression.

1 Department of Neurology, New York University Langone Health, New York, NY 10016, USA

2 Center for Dementia Research, Nathan S. Kline Institute, Orangeburg, New York 10962, USA

3 Department of Psychiatry, New York University Langone Health, New York, NY 10016, USA

4 Division of Neurochemistry, Nathan S. Kline Institute, Orangeburg, New York 10962, USA

5 Division of Analytical Psychopharmacology, Nathan S. Kline Institute, Orangeburg, New York 10962, USA

6 NYU Neuroscience Institute, New York University Langone Health, New York, NY 10016, USA

7 Department of Neuroscience and Physiology, New York University Langone Health, New York, NY 10016, USA

8 Department of Biochemistry and Molecular Pharmacology, New York University Langone Health, New York, NY 10016, USA

Correspondence to: Efrat Levy

140 Old Orangeburg Rd., Orangeburg, New York 10962, USA

E-mail: Efrat.Levy@nki.rfmh.org

Correspondence may also be addressed to: Paul Mathews
E-mail: Paul.Mathews@nki.rfmh.org

Keywords: APOE4; Alzheimer's disease; exosomes; endosomes; extracellular vesicles

Abbreviations: ALIX = apoptosis-linked gene 2-interacting protein X; ESCRT = endosomal sorting complexes required for transport

Introduction

Apolipoprotein E-mediated transport of cholesterol from astrocytes to neurons is crucial for the maintenance of synaptic connections and neuronal membranes (Pfrieger, 2003; Liu *et al.*, 2013). There are three major alleles of the apolipoprotein E (*APOE*) gene that codes for apolipoprotein E in humans— $\epsilon 2$, $\epsilon 3$, and $\epsilon 4$ (*APOE2*, *APOE3*, and *APOE4*, respectively)—with an approximate worldwide distribution of 7%, 79%, and 14%, respectively (Bertram *et al.*, 2010). Expression of *APOE4* has profound consequences within the brain, including greatly increased Alzheimer's disease risk as well as neurological effects that are independent of the hallmark Alzheimer's disease pathologies of amyloid- β plaques or neurofibrillary tangles (Liu *et al.*, 2013; Shi *et al.*, 2014). In the absence of a dementia diagnosis, human *APOE4* carriers may still display cognitive decline and olfactory identification impairments compared to age-matched non-carriers (Olofsson *et al.*, 2010; Wisdom *et al.*, 2011). Brain imaging studies also reveal *APOE4*-driven structural and functional differences within regions of the hippocampus and cortex at ages before *APOE4*-mediated Alzheimer's disease would be expected (Bookheimer and Burggren, 2009; Filippini *et al.*, 2009; Sheline *et al.*, 2010; Di Battista *et al.*, 2016), with some studies ruling out amyloid- β burden as a contributing factor (Sheline *et al.*, 2010). The idea that *APOE4* expression has deleterious effects on the brain outside of its impact on hallmark Alzheimer's disease pathologies is further supported by studies using humanized *APOE* mouse models that do not develop amyloid- β plaques or neurofibrillary tangles (Sullivan *et al.*, 1997; Tai *et al.*, 2011). *APOE4* mice show memory impairments in the Morris water maze (Andrews-Zwilling *et al.*, 2010), which have been suggested to result from regional cell loss (Tong *et al.*, 2016). Moreover, we have recently linked olfactory memory impairments in *APOE4* mice to network abnormalities in olfactory brain regions (Peng *et al.*, 2017). While the mechanisms by which *APOE4* genotype compromises neuronal viability and function are likely to be multifactorial, recent studies show that a main mechanism may be the *APOE4*-driven dysfunction of the neuronal endosomal-lysosomal system (Nuriel *et al.*, 2017; Zhao *et al.*, 2017).

Apolipoprotein E-transported cholesterol is made available to neurons upon release into early endosomes after receptor-mediated internalization, where the cholesterol is then delivered to late endosomes/multivesicular bodies (Ikonen, 2008). Within multivesicular bodies, intraluminal

vesicles are generated in a process that is mediated by the endosomal sorting complexes required for transport (ESCRT) machinery, which includes the tumor susceptibility 101 (TSG101) gene subunit and its associated protein apoptosis-linked gene 2-interacting protein X (ALIX; encoded by *PDCD6IP*) (Raiborg and Stenmark, 2009). Intraluminal vesicles are either degraded in lysosomes or released to the extracellular space as exosomes, which requires the function of small Rab-GTPases such as Rab35 for the fusion of intraluminal vesicle-containing multivesicular bodies with the cell plasma membrane (Hsu *et al.*, 2010; Ostrowski *et al.*, 2010). Exosomes play diverse physiological roles in the brain, contributing to both synaptic plasticity and neuronal survival (Rajendran *et al.*, 2014; Levy, 2017). In addition to the beneficial cell-to-cell delivery of RNA, proteins, and lipids (Rajendran *et al.*, 2014; Levy, 2017), exosomes may also contribute to the cell-to-cell and cell-to-extracellular space spread of pathogenic proteins (Levy, 2017). Importantly, exosome secretion offers a mechanism, in addition to lysosomal degradation, for the removal of intracellular materials from the endosomal system (Levy, 2017). Given that *APOE4* genotype is linked to neuronal endosome morphological alterations in human Alzheimer's disease brains (Cataldo *et al.*, 2000), that *APOE4* genotype in mouse models is sufficient to alter early endosomes and lysosomes (Nuriel *et al.*, 2017; Zhao *et al.*, 2017), and that cholesterol has been implicated in intraluminal vesicle biogenesis (Strauss *et al.*, 2010), we sought to determine whether exosome production from the endosomal pathway is disrupted by *APOE4*.

We demonstrate *APOE4*-driven decreases in exosome levels in the post-mortem brains of neuropathologically healthy humans as well as in an age-dependent manner in *APOE* mice. We further reveal differences in the levels of key exosomal-pathway regulatory proteins as well as of brain-exosome lipids, demonstrating that *APOE4* compromises brain exosome production in a manner that may be linked to *APOE4*-mediated changes in cholesterol levels. Alongside recent reports from our group (Nuriel *et al.*, 2017) and others (Zhao *et al.*, 2017), the present findings demonstrate that *APOE4* genotype disrupts exosome production in the context of broad neuronal endosomal-lysosomal pathway alterations. We propose that exosomal pathway dysfunction is an integral component of *APOE4*-driven endosomal-lysosomal pathway alterations that are likely to contribute to ageing-dependent neuron vulnerability, cognitive impairment, and Alzheimer's disease risk.

Materials and methods

Animals

All experimental procedures involving animals were approved by and complied with the guidelines of the Institutional Animal Care and Use Committee of the Nathan S. Kline Institute. The mice used in this study were from our long-standing colonies. APOE targeted-replacement mice were originally developed on a C57Bl/6 background to express human APOE3 or APOE4 genes, in place of the mouse *ApoE* gene, under the control of the endogenous murine promoter (Sullivan *et al.*, 1997). Mice homozygous for either the human APOE3 or the human APOE4 genes are referred to in the text as APOE3 and APOE4 mice, respectively. Heterozygous mice expressing one copy of human APOE3 and one copy of human APOE4 are referred to as APOE3/E4 mice. Mice were group housed under controlled temperature and lighting conditions with same-sex littermates and given free access to food and water. Mice were investigated at 6, 12, and 18 months of age as indicated. Approximately equal cohorts of males and females were examined; analysis of data by sex in this study did not reveal significant differences, and the results were pooled. Genotypes were confirmed by restriction fragment length polymorphism (RFLP) analysis following PCR, as previously described (Hixson and Vernier, 1990).

Human brain tissue preparation

Formalin-fixed and corresponding blocks of frozen (−80°C) post-mortem brain tissues from Brodmann area 9/10 of healthy controls with no neuropathological diagnoses were kindly provided by the Emory Alzheimer's Disease Research Center of the Center for Neurodegenerative Disease brain and tissue bank, under the direction of Dr Marla Gearing (see Table 1 for genotype, age at death, post-mortem interval, and diagnosis). Genotypes were confirmed by RFLP analysis following PCR, as described previously (Hixson and Vernier, 1990; Gearing *et al.*, 1995). To confirm that amyloid-β was

not present in the cases and region examined, two paraffin sections from each fixed block of brain tissue were stained with 1% thioflavin-S (Millipore Sigma) in parallel with sections from a patient with Alzheimer's disease as a positive control. On average >10 thioflavin-S positive plaques sized at ~30 μm in diameter were detected in the positive Alzheimer's disease control in a 1 mm field of view. In contrast, no plaques were detected in any brain tissues used in this study.

Extracellular vesicles isolation from the brain extracellular space

Extracellular vesicles from frozen human tissue as well as from frozen murine right hemibrains (without the cerebellum and olfactory bulbs) were isolated by serial centrifugation and purified on a sucrose gradient, as we have described previously in detail (Perez-Gonzalez *et al.*, 2012, 2017). Human extracellular vesicles were simultaneously isolated from the brain of an APOE4 carrier and an age-matched APOE3 homozygous individual. Mouse extracellular vesicles were isolated simultaneously from APOE3, APOE4 and APOE3/E4 brain tissue in aged-matched cohorts. Briefly, minced tissue was treated with papain (20 units/ml; Worthington) in 3.5 ml Hibernate A (BrainBits) at 37°C for 15 min. The enzymatic papain reaction was stopped with 6.5 ml of cold Hibernate A supplemented with protease inhibitors. Samples were serially spun at 300g at 4°C for 10 min, then 2000g for 10 min, and finally 10 000g for 30 min to pellet and discard cell debris. Extracellular vesicles were pelleted by spinning the resulting supernatants at 100 000g for 1 h. Extracellular vesicle pellets were resuspended in phosphate-buffered saline (PBS) supplemented with protease inhibitors and purified through step-wise sucrose gradients, ranging from 2 M to 0.25 M sucrose, that were spun for 16 h at 4°C at 200 000g. Seven fractions (corresponding to fractions a–g in the text) were collected, starting from the top of the sucrose gradient. Extracellular vesicles were pelleted from these fractions by spinning at 100 000g for 1 h at 4°C after dilution in PBS. Pellets were resuspended in cold PBS supplemented with protease inhibitors and lysed with RIPA buffer supplemented with protease inhibitors prior to protein

Table 1 APOE3, APOE3/E4 and APOE4 human brain samples used in this study

APOE genotype	Age at death, y	Post-mortem interval (h)	Race/sex	Braak Stage	Neuropathological diagnosis	
					Primary	Secondary
E3/3	74	7	C/f	II	Control	-
E3/3	46	6.5	C/f	0	Control	-
E3/3	65	6	C/f	II	Control	-
E3/3	57	10	C/m	II	Control	-
E3/3	75	17	C/m	I	Control	Coronary artery disease
E3/3	65	19	C/f	0	Control	Metastatic ovarian cancer
E3/3	98	15	C/m	I	Control	-
E3/4	90	6	C/m	II	Control	Congestive heart failure
E3/4	52	3	C/f	0	Control	Diffuse plaques
E3/4	60	8	AA/f	I	Control	-
E4/4	64	17	C/f	II	Control	Cerebral amyloid angiopathy
E4/4	53	6.5	AA/m	II	Control	-

Race: AA = African American; C = Caucasian; sex: m = male; f = female.

and western blot analyses (Perez-Gonzalez *et al.*, 2012, 2017). Protein levels of each extracellular vesicle-containing sucrose fraction were quantified using a BCA (bicinchoninic acid) Protein Assay Kit (Thermo Fisher Scientific). Extracellular vesicle protein levels were normalized to the weight of the brain tissue from which the extracellular vesicles were isolated.

Electron microscopy

Isolated extracellular vesicles were diluted 1/10 in 2% paraformaldehyde in 0.1 M sodium cacodylate buffer. Formvar covered carbon-coated copper 200-mesh grids were glow discharged in a Pelco easiGlow™. The extracellular vesicle-containing solution (3 μ l) was added to a grid, held by self-clamping tweezers, and left for 20 s. The solution was then wicked off with Whatman™ filter paper and negatively stained using 5 μ l of 1% uranyl acetate solution before being immediately wicked off using filter paper. This process was repeated three times before a final incubation of 5 min. The excess solution was wicked off and the grid allowed to air dry. Imaging took place on a Thermo Fisher Talos L120C transmission electron microscope operating at 120 kV.

Lipid analysis

Extracellular vesicle lipid analysis was done using fresh hemibrain tissue, which was otherwise prepared identically to frozen brain tissue. Extracellular vesicle-containing fractions and brain homogenates were lyophilized and resuspended in methyl tert-butyl ether/methanol (1:1). Samples were centrifuged at 500g for 5 min and the lipid-containing supernatant extracted. The resulting delipidated extracellular vesicle pellets were solubilized in RIPA buffer and set aside for western blot analysis. Additional methyl tert-butyl ether and water were added to the supernatant to make a mixture of methanol, methyl tert-butyl ether, and water (1:3:1) that was partitioned into water and organic phases (Matyash *et al.*, 2008). Gangliosides in the water phase were separated by high-performance thin-layer chromatography (HPTLC) using a solvent system, chloroform/methanol/0.2% CaCl₂ (60:40:9), stained with an orcinol reagent, and the amount of each ganglioside was determined as described (Saito *et al.*, 2015). The upper organic methyl tert-butyl ether phase was evaporated to dryness and separated into neutral and acidic lipids using DEAE Sephadex® columns (Macala *et al.*, 1983). The neutral lipid fraction containing ceramide and cholesterol were applied on HPTLC plates and developed first with hexane/ethyl acetate/water/acetic acid (3:4:5:2) until the solvent front ascended to 4 cm from origin, and second with hexane/methyl tert-butyl ether/acetic acid (98:2:1) until 9 cm above origin. The plate was then stained with 0.0001% primuline (Millipore Sigma), the fluorescent lipid bands were scanned with the Gel Logic molecular imaging system, and the amounts of cholesterol and ceramide were determined as described previously (Saito *et al.*, 2015).

Western blot analysis

Western blot analysis of mouse tissue was performed on extracellular vesicle fractions from the right hemibrain and parallel homogenates prepared from the left hemibrain. Human tissue western blot analysis was performed on extracellular vesicle

fractions and brain homogenates that were prepared from adjacent frozen blocks of tissue. There were no statistical differences in protein band intensities between delipidated samples and untreated samples in any of our analyses, and the data were pooled. Proteins were separated by electrophoresis with Criterion™ 4–20% Tris-HCl gel electrophoresis gels (Bio-Rad) and transferred onto PVDF (polyvinylidene difluoride) membranes (Millipore Sigma). Membranes were incubated with antibodies against the exosomal markers ALIX (1:500, Millipore Sigma #ABC40), TSG101 (1:350, GeneTex Inc #GTX70255), Rab35 (1:1000, Cell Signaling #9690S), or β -actin (1:2500, Abcam #ab8226) overnight, and horseradish peroxidase-coupled secondary antibodies for 1 h. The membranes were incubated in chemiluminescent fluid (Pierce) for 5 min, and chemiluminescence was visualized on reflection autoradiography film. Protein band density was quantified using ImageJ (NIH, Bethesda, MD) and normalized to brain tissue weight.

Quantification of mRNA levels

Quantitative PCR was performed on left hemibrains of *APOE* mice with RNA purified using the miRNeasy mini kit (Qiagen). Subsequent validation was done for quality and quantity utilizing RNA 6000 Nano (Agilent). RNA was reverse transcribed using random hexamers as described previously (Ginsberg *et al.*, 2012). TaqMan™ qPCR primers (Life Technologies) were used with samples assayed on a real-time qPCR cyclor (7900HT, Life Technologies) in 96-well optical plates with coverfilm as described previously (Ginsberg *et al.*, 2012). Standard curves and cycle threshold were generated using standards obtained from total mouse brain RNA. The ddCT method was used to determine relative gene level differences between *APOE3* and *APOE4* mice (Alldred *et al.*, 2008). Succinate dehydrogenase complex flavoprotein subunit A (*Sdha*, Mm01352360_m1) qPCR product was used as a control housekeeping gene. Negative controls consisted of the reaction mixture without input RNA and reaction mixture without SuperScript® III enzyme. *APOE3* and *APOE4* were compared with respect to the PCR product synthesis of *Tsg101* (Mm00649956_mH), *Pdcd6ip* (Mm00478041_m1) and *Rab35* (Mm01204416_m1) genes.

Statistical analysis

Western blots were quantified using NIH ImageJ (<http://rsb.info.nih.gov>). Extracellular vesicle data from mice were analysed using a repeated measures 2 \times 3 ANOVA (genotype \times age). Two-tailed *t*-tests assuming equal variance were used to make *post hoc* pair-wise genotype comparisons. Throughout, results are expressed as the mean \pm standard error of the mean (SEM). Statistically significant findings are indicated as shown: **P* < 0.05, ***P* < 0.01, and ****P* < 0.001. Dots indicate individual data points. The value of *n* represents the number of animals and is given in the main text. For qPCR, the product synthesis for each gene was modelled as a function of mouse genotype, using mixed effects models with random mouse effect to account for the correlation between repeated assays on the same mouse. The product synthesis of *Tsg101*, *Pdcd6ip*, and *Rab35* were normalized to the qPCR product of the housekeeping gene *Sdha*.

Data availability

The authors confirm that the data supporting the findings of this study are available within the article and its Supplementary material.

Results

Apolipoprotein E4 expression leads to lower brain exosome levels

To determine the effect of *APOE4* genotype on exosomes, we isolated extracellular vesicles from brains using serial centrifugations and sucrose gradients as described previously (Perez-Gonzalez *et al.*, 2012, 2017). Electron microscopy was used to confirm that extracellular vesicles were only present at sucrose gradient densities ranging from 1.09 to 1.17 g/ml (fractions b–d) and that the isolated extracellular vesicles were consistent in size and morphology with exosomes (Fig. 1) (Perez-Gonzalez *et al.*, 2012). There were no noticeable differences in extracellular vesicle size or

morphology by electron microscopy when comparing the extracellular vesicle-containing fractions (fractions b–d) or when comparing extracellular vesicles isolated from *APOE3* homozygous, *APOE3/E4* heterozygous, and *APOE4* homozygous mice (Fig. 1).

Human brain tissue for extracellular vesicle isolation was from individuals with ages that ranged from 46 to 98 years of age (Table 1), with a mean age of 68.6 ± 6.18 years for *APOE3* homozygous individuals and 63.8 ± 6.92 years for *APOE4* carriers. Frontal cortices of *APOE4* carriers (either *APOE4* homozygous or *APOE3/E4* heterozygous) contained significantly lower levels of extracellular vesicles than those of non-carriers (*APOE3* homozygous) as determined by total extracellular vesicle protein levels pooled from fractions b–d normalized to brain tissue weight [$46.9 \pm 9.0\%$ of *APOE3* individuals; $n=7$ *APOE3*, $n=5$ *APOE4* carriers, $t(10)=3.26$, $P=0.009$; Fig. 2A]. Levels of flotillin-1, a lipid-raft protein present in all extracellular vesicle subtypes (Kowal *et al.*, 2016), were not significantly different in extracellular vesicles isolated from *APOE4* carriers compared with *APOE3* brains [$n=3$ for both genotypes, $t(4)=0.85$, $P=0.45$; Fig. 2B and C]. While brain

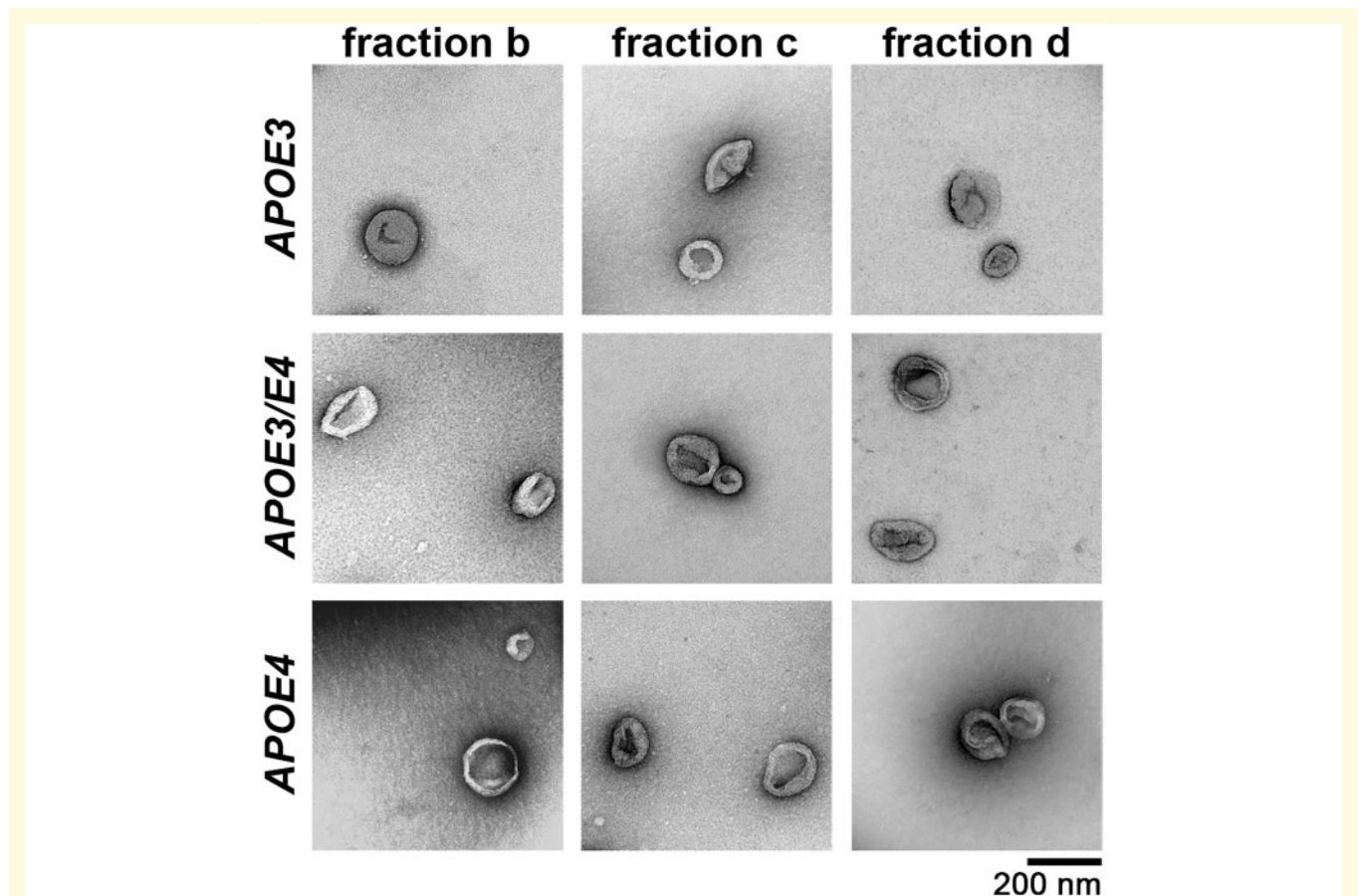


Figure 1 Electron microscopy shows appropriately sized and shaped extracellular vesicles isolated from the brains of *APOE* mice. Wide field electron microscopy imaging shows extracellular vesicles isolated from the brains of 12-month-old *APOE3*, *APOE3/E4*, and *APOE4* mice. No obvious differences were observed in size or morphology among the genotypes and among the three extracellular vesicle-containing fractions b–d.



Figure 2 Brain extracellular vesicle protein levels are lower in human *APOE4*-carriers compared with homozygous *APOE3* individuals.

(A) Extracellular vesicle protein levels from human brains normalized to brain tissue weight. (B) A representative western blot showing ALIX and TSG101 (exosomal proteins), and flotillin-1 (a lipid-raft enriched protein) in the extracellular vesicles. (C) Quantification of band intensities normalized to brain tissue weight is shown for levels of ALIX, TSG101, and flotillin-1. Data are expressed as the mean \pm SEM of the ratios of *APOE4* carriers to *APOE3*. * $P < 0.05$, ** $P < 0.01$.

extracellular vesicles isolated by our protocol are primarily exosomes, other extracellular vesicles such as microvesicles may co-purify (Cocucci and Meldolesi, 2015). We therefore examined levels of the proteins ALIX and TSG101, exosome-specific ESCRT components that are commonly used as exosome markers, in our extracellular vesicle fractions to determine if *APOE4* expression specifically affects exosome levels (Fig. 2B and C). Lower levels in fractions b–d normalized to brain tissue weight were revealed for both ALIX [$40.02 \pm 12.2\%$ of *APOE3* individuals; $n = 4$, $t(6) = 2.99$, $P = 0.02$] and TSG101 [$52.8 \pm 3.6\%$ of *APOE3* individuals; $n = 4$, $t(7) = 2.98$, $P = 0.02$] in *APOE4* carriers compared with *APOE3* by western blot analyses (Fig. 2B and C). Thus, we show that exosome levels are reduced in *APOE4*-expressing human brains.

To determine that the observed effects on exosome levels are solely dependent on *APOE* genotype, we isolated brain extracellular vesicles from humanized *APOE* homozygous mice that do not develop tau or amyloid- β pathology (Sullivan *et al.*, 1997; Tai *et al.*, 2011). Data from sucrose gradient fractions b–d were pooled for all analyses. Repeated measures 2×3 ANOVA (genotype \times age) revealed a main effect of genotype [$F(1,78) = 9.37$, $P = 0.003$], but not age independent of genotype [$F(2,78) = 0.19$, $P = 0.82$], on brain extracellular vesicle total protein levels. In agreement with our human findings, *post hoc t*-test analysis between groups showed lower extracellular vesicle protein levels in the right hemibrains of 12-month-old [$88.2 \pm 2.1\%$ of *APOE3* levels; $n = 18$, $t(34) = 3.3$, $P = 0.002$; Fig. 3A] and 18-month-old [$91.4 \pm 1.5\%$ of *APOE3* levels; $n = 10$ *APOE3*, $n = 11$ *APOE4*, $t(19) = 3.14$, $P = 0.005$; Fig. 3A] *APOE4* compared with age-matched *APOE3* mice. Six-month-old *APOE4* mice showed no difference in brain extracellular vesicle protein levels when compared with age-matched *APOE3* mice [$n = 13$ *APOE3*, $n = 14$ *APOE4*, $t(25) = 0.98$, $P = 0.33$; Fig. 3A], indicating that the *APOE4* effect on brain extracellular vesicles is age-dependent. Levels of flotillin-1 were not found to differ by *APOE* genotype at any age by *t*-test analyses [6-month-old $n = 5$, $t(8) = 1.67$, $P = 0.13$; 12-

month-old $n = 5$, $t(8) = 0.48$, $P = 0.64$; 18-month-old $n = 5$, $t(8) = 2.31$, $P = 0.18$; Fig. 3B and E]. Exosome-specific markers were examined in extracellular vesicle fractions to confirm that brain exosome levels were specifically affected by *APOE4* expression (Fig. 3B). Repeated measures 2×3 ANOVA (genotype \times age) revealed a main effect by genotype with significant interaction with age for both ALIX [genotype $F(1,46) = 8.79$, $P = 0.004$; interaction $F(2,46) = 8.55$, $P = 0.0007$] and TSG101 [genotype $F(1,30) = 5.99$, $P = 0.02$; interaction $F(2,30) = 7.05$, $P = 0.003$]. *Post hoc t*-test analyses between groups revealed that ALIX and TSG101 levels in the brain extracellular vesicles of *APOE4* mice were lower at both 12 [ALIX $59.7 \pm 4.8\%$ of *APOE3*; $n = 12$, $t(22) = 3.89$, $P = 0.0007$; TSG101 $82.8 \pm 4.8\%$ of *APOE3*; $n = 6$, $t(10) = 2.34$, $P = 0.04$] and 18 months of age [ALIX $62.4 \pm 8.6\%$ of *APOE3*; $n = 5$, $t(8) = 3.10$, $P = 0.02$; TSG101 $60.5 \pm 6.6\%$ of *APOE3*; $n = 6$, $t(10) = 4.23$, $P = 0.002$] when normalized to brain tissue weight (Fig. 3C and D). ALIX and TSG101 levels did not differ in the brain extracellular vesicles of 6-month-old *APOE4* compared with *APOE3* mice [ALIX $n = 9$, $t(16) = 1.58$, $P = 0.13$; TSG101 $n = 6$, $t(10) = 1.13$, $P = 0.29$; Fig. 3C and D].

Given that our human *APOE4* findings are from both homozygous *APOE4* and heterozygous *APOE3/E4* individuals (Fig. 2), we repeated a study of 12-month-old mice with the addition of heterozygous *APOE3/E4* mice (Fig. 4). These additional data confirmed that 12-month-old *APOE4* compared with *APOE3* mice showed significantly lower extracellular vesicle levels of total protein [$86.6 \pm 4.1\%$ of *APOE3*; $n = 10$ *APOE3*, $n = 8$ *APOE4*, $t(16) = 2.21$, $P = 0.04$], ALIX [$64.5 \pm 14.9\%$ of *APOE3*; $n = 7$ *APOE3*, $n = 6$ *APOE4*, $t(11) = 2.59$, $P = 0.03$], and TSG101 [$68.1 \pm 15.1\%$ of *APOE3*; $n = 6$ *APOE3*, $n = 5$ *APOE4*, $t(9) = 2.34$, $P = 0.04$] (Fig. 4). In these groups, 12-month-old *APOE4* compared with *APOE3* mice additionally showed significantly lower extracellular vesicle levels of flotillin-1 [$70.0 \pm 10.5\%$ of *APOE3*; $n = 7$, $t(12) = 2.56$, $P = 0.02$] (Fig. 4B and E). Analysis of extracellular vesicles isolated from the brains of 12-month-old *APOE3/E4* compared

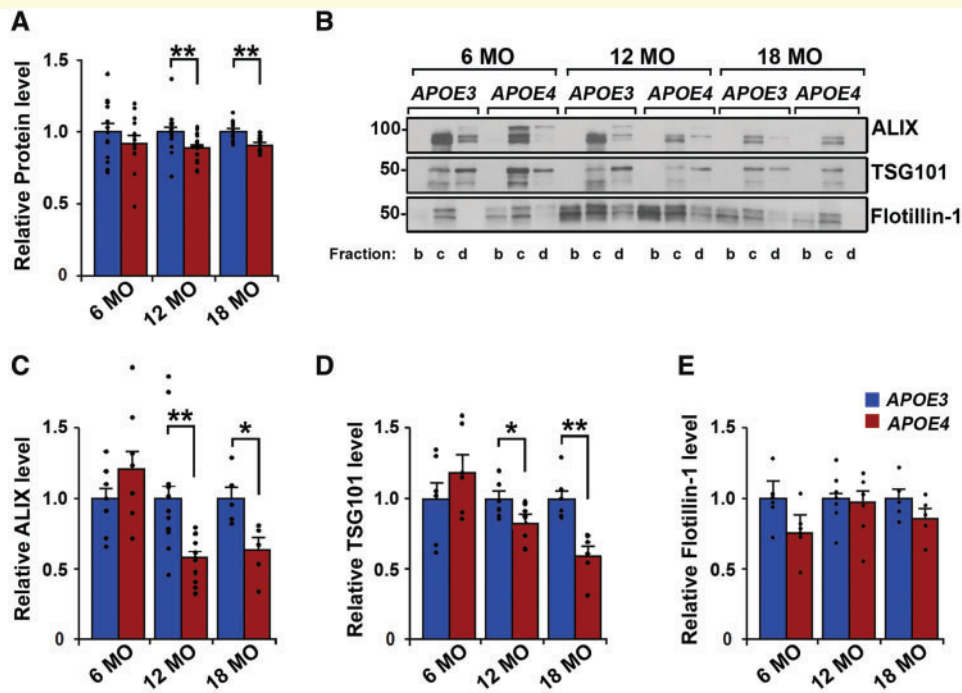


Figure 3 Brain exosome levels are lower in APOE4 compared with APOE3 mice in an age-dependent manner. (A) Protein levels in sucrose gradient fractions b–d from each age group are shown for extracellular vesicles isolated from mouse hemibrains normalized to hemibrain weight. (B) ALIX, TSG101, and flotillin-1 were analysed by western blotting. Quantification of band intensities normalized to initial hemibrain weight are shown for levels of ALIX (C), TSG101 (D), and flotillin-1 (E). Data are expressed as the mean \pm SEM of the ratios of APOE4 to APOE3. * $P < 0.05$, ** $P < 0.01$.

with APOE3 mice revealed significantly lower levels of ALIX [$58.1 \pm 19.0\%$ of APOE3, $n=7$, $t(12)=2.18$, $P = 0.048$] (Fig. 4B and C). Lower but not significant levels were also detected for total extracellular vesicle protein [$92.8 \pm 4.1\%$ of APOE3; $n=10$, $t(18)=1.37$, $P = 0.19$], flotillin-1 [$71.0 \pm 14.3\%$ of APOE3; $n=7$, $t(12)=1.91$, $P = 0.08$], and TSG101 [$73.7 \pm 12.4\%$ of APOE3; $n=6$, $t(10)=2.12$, $P = 0.06$] in the brain extracellular vesicles of 12-month-old APOE3/E4 compared with APOE3 mice (Fig. 4). That these exosome marker levels in 12-month-old APOE3/E4 mice brains were either significantly lower than in age-matched APOE3 mice, or intermediate between the levels found in age-matched APOE3 and APOE4 mice, suggests that 12 months is a critical age when mechanisms of exosomal production and release begin to decline in APOE4 carriers and that this decline may be gene-dose sensitive. Altogether, our findings indicate that APOE4 expression leads to lower exosome levels in the brains of both humans and APOE mice, with the mice data further suggesting that the effect is ageing-dependent.

Exosomal formation and secretion are downregulated in aged APOE4 compared with APOE3 mouse brains

To determine whether APOE genotype-mediated differences in brain exosome levels are due to altered exosome

biogenesis and/or secretion, we examined the expression of intraluminal vesicle formation regulators (ALIX and TSG101) as well as a regulator of multivesicular body fusion with the plasma membrane (Rab35) (Raiborg and Stenmark, 2009; Hsu *et al.*, 2010) in the brains of APOE mice (Fig. 5). From the same mice in which extracellular vesicles were isolated from the right hemibrain, left hemibrain homogenates were used to measure protein expression levels of ALIX, TSG101, and Rab35. Repeated measures ANOVA (genotype \times age) on hemibrain protein levels revealed a main effect of genotype for TSG101 [$F(1,50)=14.14$, $P = 0.0004$], as well as of genotype and age with significant interaction for Rab35 [genotype $F(1,64)=5.32$, $P = 0.02$; age $F(2,64)=4.88$, $P = 0.01$; interaction $F(2,64)=4.86$, $P = 0.01$]. *Post hoc t*-tests between groups revealed that TSG101 levels were reduced in APOE4 compared with APOE3 mice at 12 [$73.4 \pm 8.4\%$ of APOE3; $n=11$ APOE3, $n=12$ APOE4, $t(21)=2.44$, $P = 0.02$] and 18 months of age [$76.6 \pm 5.8\%$ of APOE3; $n=14$ APOE3, $n=13$ APOE4, $t(25)=3.16$, $P = 0.004$; Fig. 5C]. Rab35 levels in APOE4 mice were significantly lower at 18 months of age [$67.4 \pm 4.7\%$ of APOE3; $n=14$ APOE3, $n=13$ APOE4, $t(25)=4.83$, $P = 0.00006$; Fig. 5D]. Consistent with the lack of exosome level differences at 6 months of age, hemibrain levels of TSG101 and Rab35 showed no significant genotype-mediated differences at this age [TSG101 $n=5$, $t(8)=1.28$, $P = 0.24$; Rab35

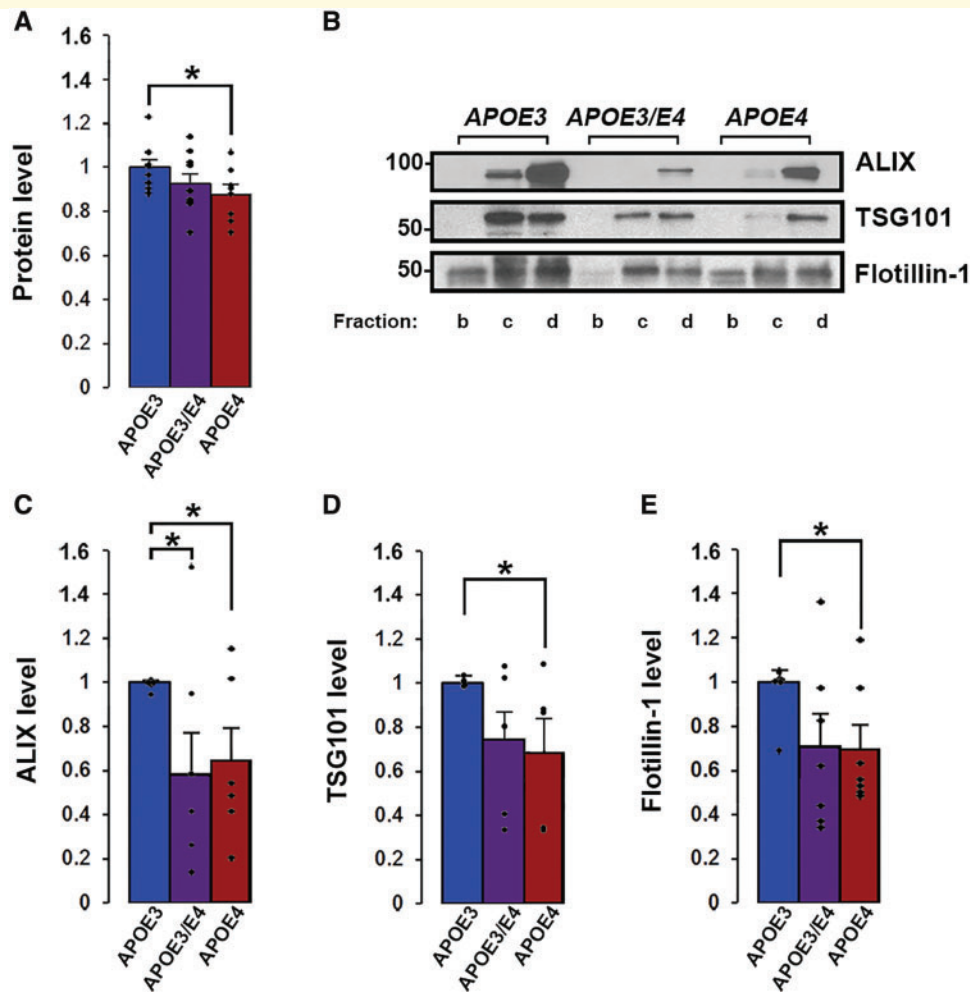


Figure 4 APOE4-driven effects on exosome levels are gene dose dependent in 12-month-old mice. (A) Protein levels in sucrose gradient fractions b–d are shown for extracellular vesicles isolated from mouse hemibrains normalized to hemibrain weight. (B) ALIX, TSG101, and flotillin-1 were analysed by western blotting. Quantification of band intensities normalized to initial hemibrain weight are shown for levels of ALIX (C), TSG101 (D), and flotillin-1 (E). Data are expressed as the mean \pm SEM of the ratios when compared with APOE3. * $P < 0.05$.

$n = 7$; $t(12) = 0.35$, $P = 0.74$; Fig. 5C and D]. ALIX levels were not significantly different in the hemibrains of APOE4 mice compared with APOE3 mice at any age [6 months old $n = 7$, $t(12) = 0.09$, $P = 0.93$; 12 months old $n = 13$ APOE3, $n = 14$ APOE4, $t(25) = 1.28$, $P = 0.21$; 18 months old $n = 16$ APOE3, $n = 15$ APOE4, $t(29) = 1.46$, $P = 0.16$; Fig. 5B]. To determine if APOE4-mediated reductions in protein levels were due to downregulated transcription, we conducted qPCR analyses for *Pdcd6ip* (encodes ALIX), *Tsg101*, and *Rab35* mRNA from the hemibrains of 12-month-old APOE mice. Brain mRNA levels were reduced for *Tsg101* [$88.8 \pm 1.9\%$ of APOE3; $n = 6$, $t(23) = 4.05$, $P = 0.0005$] and *Rab35* [$87.3 \pm 2.2\%$ of APOE3; $n = 6$, $t(25) = 4.24$, $P = 0.0003$] in APOE4 compared with APOE3 mice, whereas *Pdcd6ip* mRNA levels were not statistically different [$91.0 \pm 4.1\%$ of APOE3; $n = 6$, $t(24) = 1.60$, $P = 0.12$; Fig. 5E]. Altogether, our findings suggest that a downregulation of molecular events involved

in exosomal biogenesis and secretion lead to the reduction of brain exosome levels in APOE4 carriers.

Lipid composition is altered in APOE4 mice exosomes

Lipids such as cholesterol, ceramides, and gangliosides are enriched in exosomal membranes when compared with other cell membranes, reflecting the unique lipid environment of multivesicular bodies (Mobius et al., 2003). We determined the concentrations of cholesterol, ceramide, and gangliosides in 12-month-old APOE mouse brains and brain extracellular vesicles. As previously reported (Mobius et al., 2003), our mouse brain extracellular vesicles were ~ 10 times as enriched in cholesterol and ~ 50 times as enriched in ceramide and gangliosides compared with total brain lipid concentrations (Fig. 6). At the

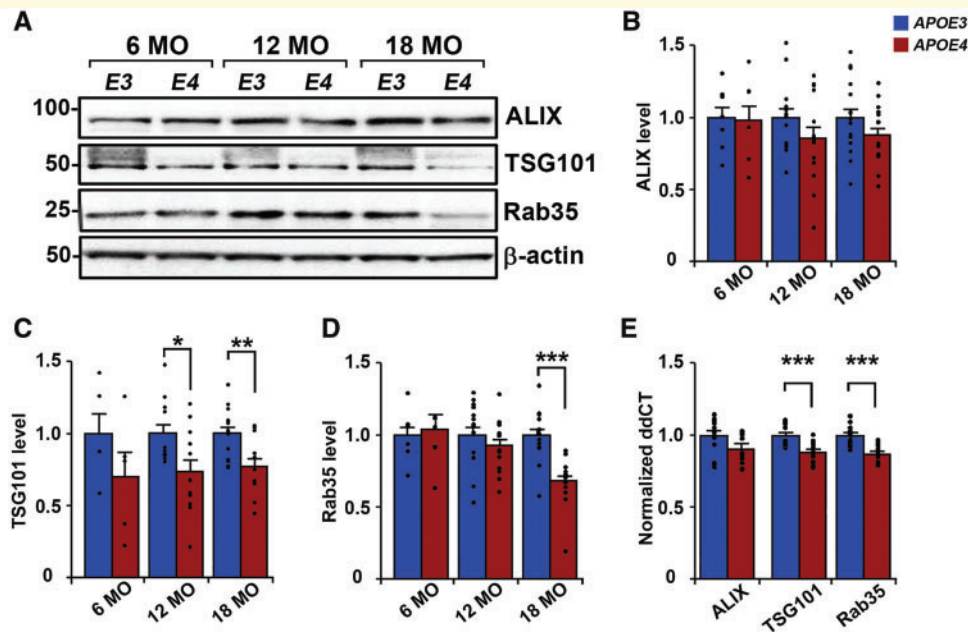


Figure 5 Expression levels of TSG101 and Rab35 are lower in aged APOE4 mouse brains compared with age-matched APOE3 mice. (A) Representative western blot analyses of mouse hemibrain homogenates are shown for ALIX, TSG101, and Rab35, with β -actin used as a loading control. (B–D) Quantification of bands normalized to levels of β -actin is shown for levels of ALIX (B), TSG101 (C), and Rab35 (D). (E) Quantitative PCR analysis of 12-month-old mouse hemibrains shows *Pdc61p* (encodes ALIX), *Tsg101*, and *Rab35* transcript levels normalized to ddCT levels of the housekeeping gene *Sdha*. Data are expressed as the mean \pm SEM of the ratios of APOE4 to APOE3. * $P < 0.05$, ** $P < 0.01$, *** $P < 0.001$.

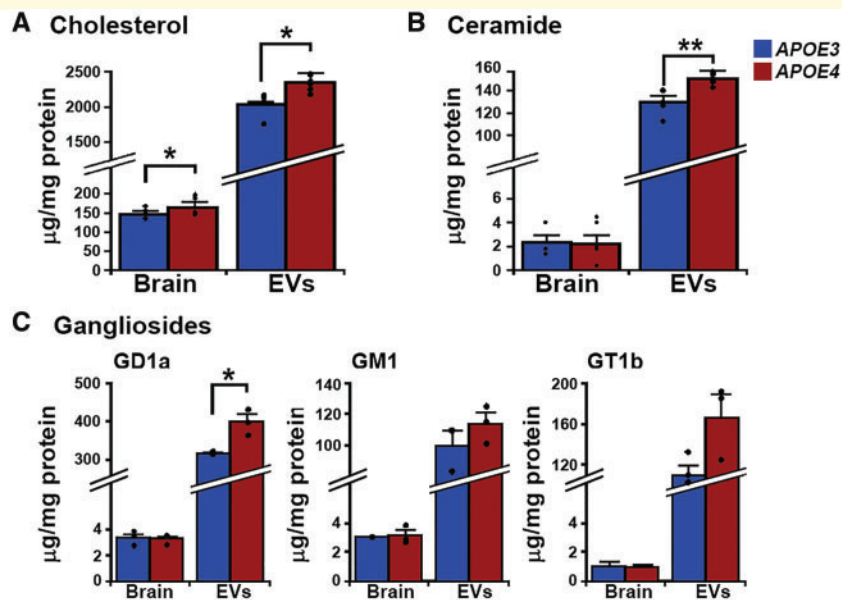


Figure 6 Differences in brain extracellular vesicle lipids in APOE4 compared with APOE3 mice. Brain and extracellular vesicle lipid concentrations are given in $\mu\text{g}/\text{mg}$ of protein for (A) cholesterol, (B) ceramide, and (C) gangliosides. Data are expressed as the mean \pm SEM. * $P < 0.05$, ** $P < 0.01$.

hemibrain level, cholesterol concentrations were higher in 12-month-old APOE4 compared with age-matched APOE3 mouse brains [$112.6 \pm 3.9\%$ of APOE3; $n = 4$ APOE3, $n = 5$ APOE4, $t(7) = 2.59$, $P = 0.04$; Fig. 6A],

while concentrations of ceramide and gangliosides did not differ (Fig. 6B and C). Cholesterol concentrations were also higher in the brain extracellular vesicles of APOE4 compared with APOE3 mice [$115.0 \pm 5.9\%$ of APOE3; $n = 5$,

$t(8)=3.38$, $P=0.01$; Fig. 6A]. Consistent with previous observations that endosomal cholesterol build-up is commonly associated with ganglioside accumulation (Lloyd-Evans and Platt, 2010), *APOE4* mouse brain extracellular vesicles had higher levels of the ganglioside-precursor ceramide [$116 \pm 4.5\%$ of *APOE3*; $n=5$, $t(8)=3.36$, $P=0.01$; Fig. 6B] as well as the ganglioside GD1a [$125.2 \pm 6.3\%$ of *APOE3*; $n=3$; $t(4)=3.97$, $P=0.02$, Fig. 6C]. These findings demonstrate that *APOE4* alters brain and extracellular vesicle cholesterol levels, with associated changes in extracellular vesicle levels of ceramide and ganglioside.

Discussion

Our findings demonstrate an *APOE4*-mediated decrease in brain exosome levels in both humans and humanized *APOE* mice, with our mouse findings showing that this is ageing-dependent, consistent with *APOE4*'s contribution to ageing-related disease risk (Mahley, 2016). Our findings further indicate that exosomal decrease follows a downregulation of exosome biogenesis and secretion from the endosomal pathway. We reveal a transcriptional and protein level downregulation of TSG101 in the brains of aged *APOE4* mice, consistent with previous findings that depleting specific ESCRT components such as TSG101 is sufficient to decrease exosome secretion *in vitro* (Colombo *et al.*, 2013). While we did not find a reduction in the brain expression of ALIX, an ESCRT-associated protein that interacts with TSG101 during intraluminal vesicular formation, this finding agrees with data from depletion studies suggesting that ALIX's contribution to exosome formation may depend on the cell type (Baietti *et al.*, 2012; Colombo *et al.*, 2013). The observed reduction in exosome secretion is additionally supported by our finding that *APOE4* downregulates Rab35, a rab GTPase that functions in the docking of multivesicular bodies to the plasma membrane for exosome release. Inhibition of Rab35 has been shown to lead to impaired exosome secretion in several *in vitro* models (Hsu *et al.*, 2010; Abrami *et al.*, 2013). Taken together, our data indicate that lower exosome levels in the brains of *APOE4* carriers are likely a consequence of downregulated exosome biogenesis and secretion rather than changes in exosome stability or clearance from the brain extracellular space.

The apolipoprotein E protein is likely to exert its effects on endosomal and exosomal pathways through its primary role as a lipid carrier, supported by studies that *APOE4* compared with *APOE3* expression disrupts neuronal and peripheral cholesterol metabolism (Sing and Davignon, 1985; Michikawa *et al.*, 2000). We found an increase in cholesterol levels in the exosomes of *APOE4* compared with *APOE3* mice that likely reflects altered lipid metabolism within the endosomal pathway from which they originate. Lipids such as cholesterol accumulate in intracellular vesicles under certain pathological conditions, such as in Alzheimer's disease and select lysosomal storage disorders

(Distl *et al.*, 2001; Kuech *et al.*, 2016). Aberrant accumulation of cholesterol, along with the secondary accumulation of sphingolipids, can cause disturbances in the endosomal pathway that affect both the morphology and motility of endosomal compartments (Lebrand *et al.*, 2002; Marquer *et al.*, 2014). For example, endosomal cholesterol accumulation has been shown to immobilize multivesicular bodies through the impaired inactivation of Rab7 (Lebrand *et al.*, 2002; Chen *et al.*, 2008). We therefore suggest that *APOE4*'s disruption of intracellular cholesterol metabolism may be directly associated with compromised exosome production. While several other members of the Rab protein family are known to be regulated by endosomal cholesterol levels (Choudhury *et al.*, 2004; Glodowski *et al.*, 2007), it remains to be determined if Rab35 function, which shows decreased levels in brains of *APOE4* mice, may also be affected by changes in cholesterol levels.

An *APOE4*-mediated alteration in brain exosome pathways introduces an additional component to the endosomal-lysosomal disruption that appears to be a prominent feature of *APOE4*-driven neuronal changes (Cataldo *et al.*, 2000; Nuriel *et al.*, 2017; Zhao *et al.*, 2017). Alzheimer's disease-related early endosome enlargement in neurons was previously shown by Cataldo *et al.* (2000) to be more prominent in *APOE4* carriers than non-carriers, including in brain regions not affected by amyloid- β pathology. More recently, 22-month-old *APOE4* mice were found to have neuronal endosomal pathology that impairs insulin signaling (Zhao *et al.*, 2017). Moreover, we have recently demonstrated with RNA sequencing that carrying an *APOE4* allele leads to robust alterations in the expression of multiples genes involved in the endosomal-lysosomal system when comparing the Alzheimer's disease-vulnerable entorhinal cortex to an Alzheimer's disease-resistant brain region (primary visual cortex) of 14 to 15-month-old *APOE* mice (Nuriel *et al.*, 2017). We additionally showed that the number and size of early endosomes is increased in cingulate cortex pyramidal neurons of *APOE4* mice at 18 months of age, but not at 12 months or earlier ages (Nuriel *et al.*, 2017). Further evidence for *APOE4*-dependent lysosomal changes comes from our findings that lysosome number is increased in the entorhinal pyramidal neurons of 18-month-old *APOE4* mice (Nuriel *et al.*, 2017). The current findings show that *APOE4*-driven brain exosome compromise at 12 months of age occurs earlier than the reported *APOE4*-driven endosome or lysosome changes, raising the possibility that reduced outward flux through the exosomal pathway might contribute to subsequent endosomal-lysosomal pathway alterations. Down syndrome patients and mouse models of the disease all show early endosome enlargement (Colacurcio *et al.*, 2017), which is also associated with a change in the exosomal pathway, albeit an increase in exosome production (Gauthier *et al.*, 2017). Importantly in this study, reducing exosome generation worsened the endosomal pathology in cultured Down syndrome fibroblasts (Gauthier *et al.*, 2017), suggesting that flux through

the exosomal pathway is an important regulator of endosomal compartments. Similarly, knockdown of TSG101 and Rab35 in cells *in vitro* has been shown to result in morphological endosomal changes in addition to downregulating exosome secretion (Razi and Futter, 2006; Allaire *et al.*, 2010). Thus, reduced exosome release in APOE4 carriers may be a contributing factor to the extensive neuronal endosomal pathway alterations that have been linked to this allele.

Our findings link the APOE4 genotype to a failure in brain exosome production in an *in vivo*, Alzheimer's disease pathology-free setting, contributing to existing evidence that the neuronal endosomal-lysosomal system is broadly disrupted in individuals expressing this allele. Disturbances of endosomal-lysosomal system function often result in the accumulation of surplus material in neuronal endosomes and lysosomes (Nixon, 2004), and disruptions throughout these pathways are an important factor contributing to neuronal vulnerability in numerous neurodegenerative disorders, including Alzheimer's disease (Nixon, 2005; Schreij *et al.*, 2016). Consistent with our findings here, we propose that endosomal material released into the extracellular space via exosomes is an important mechanism by which neurons remove debris, and that failure of efficient exosome production and release can exacerbate and perhaps lead to endosomal pathway disturbances (Gauthier *et al.*, 2017). This failure to maintain proper functioning of the neuronal endosomal-lysosomal and exosomal pathways in APOE4 carriers during ageing may not only disturb essential homeostatic and catabolic cellular processes, but may also contribute to neuronal vulnerability and the risk of developing neurodegenerative disorders such as Alzheimer's disease (Nixon, 2017).

Acknowledgements

We thank Dr. Monika Pawlik for her expert assistance with our mouse colonies, and Sang Han Lee at the Center for Biomedical Imaging and Neuromodulation at the Nathan S. Kline Institute for the statistical analysis of the qPCR data. Human tissue was kindly provided by the Emory ADRC/CND under the direction of Dr. Marla Gearing.

Funding

This work was supported by the NIH (P01 AG017617 and R01 AG057517 to P.M.M. and E.L., and R01 AG043375 and P01 AG014449 to S.D.G.). K.P. was additionally supported by NIH predoctoral and postdoctoral research training grants (T32-GM066704, Dr. Erika Bach; T32-AG052909, Drs Thomas Wisniewski and Helen Scharfman) and the Sackler Institute of Graduate Biomedical Sciences, New York University School of Medicine. The provision of human tissue from the Emory

ADRC/CND was supported by the NIH (AG025688 to Dr. Marla Gearing). The funding sources were not involved in the study design; in the collection, analysis and interpretation of data; in the writing of the report; or in the decision to submit the article for publication.

Competing interests

The authors report no competing interests.

Supplementary material

Supplementary material is available at *Brain* online.

References

- Abrami L, Brandi L, Moayeri M, Brown MJ, Krantz BA, Leppla SH, et al. Hijacking multivesicular bodies enables long-term and exosome-mediated long-distance action of anthrax toxin. *Cell Rep* 2013; 5: 986–96.
- Allaire PD, Marat AL, Dall'Armi C, Di Paolo G, McPherson PS, Ritter B. The Connecdenn DENN domain: a GEF for Rab35 mediating cargo-specific exit from early endosomes. *Mol Cell* 2010; 37: 370–82.
- Allred MJ, Che S, Ginsberg SD. Terminal Continuation (TC) RNA amplification enables expression profiling using minute RNA input obtained from mouse brain. *Int J Mol Sci* 2008; 9: 2091–104.
- Andrews-Zwilling Y, Bien-Ly N, Xu Q, Li G, Bernardo A, Yoon SY, et al. Apolipoprotein E4 causes age- and Tau-dependent impairment of GABAergic interneurons, leading to learning and memory deficits in mice. *J Neurosci* 2010; 30: 13707–17.
- Baietti MF, Zhang Z, Mortier E, Melchior A, Degeest G, Geeraerts A, et al. Syndecan-syntenin-ALIX regulates the biogenesis of exosomes. *Nat Cell Biol* 2012; 14: 677–85.
- Bertram L, McQueen MB, Mullin K, Blacker D, Tanzi RE. The AlzGene Database. *Alzheimer Research Forum*, January 29, 2010. Available from: <http://www.alzgene.org> (1 June 2017, date last accessed)
- Bookheimer S, Burggren A. APOE-4 genotype and neurophysiological vulnerability to Alzheimer's and cognitive aging. *Annu Rev Clin Psychol* 2009; 5: 343–62.
- Cataldo AM, Peterhoff CM, Troncoso JC, Gomez-Isla T, Hyman BT, Nixon RA. Endocytic pathway abnormalities precede amyloid beta deposition in sporadic Alzheimer's disease and Down syndrome: differential effects of APOE genotype and presenilin mutations. *Am J Pathol* 2000; 157: 277–86.
- Chen H, Yang J, Low PS, Cheng JX. Cholesterol level regulates endosome motility via Rab proteins. *Biophys J* 2008; 94: 1508–20.
- Choudhury A, Sharma DK, Marks DL, Pagano RE. Elevated endosomal cholesterol levels in Niemann-Pick cells inhibit rab4 and perturb membrane recycling. *Mol Biol Cell* 2004; 15: 4500–11.
- Cocucci E, Meldolesi J. Ectosomes and exosomes: shedding the confusion between extracellular vesicles. *Trends Cell Biol* 2015; 25: 364–72.
- Colacurcio DJ, Pensalfini A, Jiang Y, Nixon RA. Dysfunction of autophagy and endosomal-lysosomal pathways: roles in pathogenesis of down syndrome and Alzheimer's Disease. *Free Radic Biol Med* 2018; 114: 40–51.
- Colombo M, Moita C, van Niel G, Kowal J, Vigneron J, Benaroch P, et al. Analysis of ESCRT functions in exosome biogenesis, composition and secretion highlights the heterogeneity of extracellular vesicles. *J Cell Sci* 2013; 126 (Pt 24): 5553–65.

- Di Battista AM, Heinsinger NM, Rebeck GW. Alzheimer's disease genetic risk factor APOE- ϵ 4 also affects normal brain function. *Curr Alzheimer Res* 2016; 13: 1200–7.
- Distl R, Meske V, Ohm TG. Tangle-bearing neurons contain more free cholesterol than adjacent tangle-free neurons. *Acta Neuropathol* 2001; 101: 547–54.
- Filippini N, MacIntosh BJ, Hough MG, Goodwin GM, Frisoni GB, Smith SM, et al. Distinct patterns of brain activity in young carriers of the APOE- ϵ 4 allele. *Proc Natl Acad Sci USA* 2009; 106: 7209–14.
- Gauthier SA, Perez-Gonzalez R, Sharma A, Huang FK, Alldred MJ, Pawlik M, et al. Enhanced exosome secretion in Down syndrome brain—a protective mechanism to alleviate neuronal endosomal abnormalities. *Acta Neuropathol Commun* 2017; 5: 65.
- Gearing M, Schneider JA, Rebeck GW, Hyman BT, Mirra SS. Alzheimer's disease with and without coexisting Parkinson's disease changes: apolipoprotein E genotype and neuropathologic correlates. *Neurology* 1995; 45: 1985–90.
- Ginsberg SD, Alldred MJ, Che S. Gene expression levels assessed by CA1 pyramidal neuron and regional hippocampal dissections in Alzheimer's disease. *Neurobiol Dis* 2012; 45: 99–107.
- Glodowski DR, Chen CC, Schaefer H, Grant BD, Rongo C. RAB-10 regulates glutamate receptor recycling in a cholesterol-dependent endocytosis pathway. *Mol Biol Cell* 2007; 18: 4387–96.
- Hixson JE, Vernier DT. Restriction isotyping of human apolipoprotein E by gene amplification and cleavage with HhaI. *J Lipid Res* 1990; 31: 545–8.
- Hsu C, Morohashi Y, Yoshimura S, Manrique-Hoyos N, Jung S, Lauterbach MA, et al. Regulation of exosome secretion by Rab35 and its GTPase-activating proteins TBC1D10A-C. *J Cell Biol* 2010; 189: 223–32.
- Ikonen E. Cellular cholesterol trafficking and compartmentalization. *Nat Rev Mol Cell Biol* 2008; 9: 125–38.
- Kowal J, Arras G, Colombo M, Jouve M, Morath JP, Prindal-Bengtson B, et al. Proteomic comparison defines novel markers to characterize heterogeneous populations of extracellular vesicle subtypes. *Proc Natl Acad Sci USA* 2016; 113: E968–77.
- Kuech EM, Brogden G, Naim HY. Alterations in membrane trafficking and pathophysiological implications in lysosomal storage disorders. *Biochimie* 2016; 130: 152–62.
- Lebrand C, Corti M, Goodson H, Cosson P, Cavalli V, Mayran N, et al. Late endosome motility depends on lipids via the small GTPase Rab7. *EMBO J* 2002; 21: 1289–300.
- Levy E. Exosomes from the diseased brain: first insights from *in vivo* studies. *Front Neurosci* 2017; 11: 142.
- Liu CC, Kanekiyo T, Xu H, Bu G. Apolipoprotein E and Alzheimer disease: risk, mechanisms and therapy. *Nat Rev Neurol* 2013; 9: 106–18.
- Lloyd-Evans E, Platt FM. Lipids on trial: the search for the offending metabolite in Niemann-Pick type C disease. *Traffic* 2010; 11: 419–28.
- Macala LJ, Yu RK, Ando S. Analysis of brain lipids by high performance thin-layer chromatography and densitometry. *J Lipid Res* 1983; 24: 1243–50.
- Mahley RW. Apolipoprotein E: from cardiovascular disease to neurodegenerative disorders. *J Mol Med* 2016; 94: 739–46.
- Marquer C, Laine J, Dauphinot L, Hanbouch L, Lemerrier-Neuillet C, Pierrot N, et al. Increasing membrane cholesterol of neurons in culture recapitulates Alzheimer's disease early phenotypes. *Mol Neurodegener* 2014; 9: 60.
- Matyash V, Liebisch G, Kurzchalia TV, Shevchenko A, Schwudke D. Lipid extraction by methyl-tert-butyl ether for high-throughput lipidomics. *J Lipid Res* 2008; 49: 1137–46.
- Michikawa M, Fan QW, Isobe I, Yanagisawa K. Apolipoprotein E exhibits isoform-specific promotion of lipid efflux from astrocytes and neurons in culture. *J Neurochem* 2000; 74: 1008–16.
- Mobius W, van Donselaar E, Ohno-Iwashita Y, Shimada Y, Heijnen HFG, Slot JW, et al. Recycling compartments and the internal vesicles of multivesicular bodies harbor most of the cholesterol found in the endocytic pathway. *Traffic* 2003; 4: 222–31.
- Nixon RA. Niemann-Pick Type C disease and Alzheimer's disease: the APP-endosome connection fattens up. *Am J Pathol* 2004; 164: 757–61.
- Nixon RA. Endosome function and dysfunction in Alzheimer's disease and other neurodegenerative diseases. *Neurobiol Aging* 2005; 26: 373–82.
- Nixon RA. Amyloid precursor protein and endosomal-lysosomal dysfunction in Alzheimer's disease: inseparable partners in a multifactorial disease. *FASEB J* 2017; 31: 2729–43.
- Nuriel T, Peng KY, Ashok A, Dillman AA, Figueroa HY, Apuzzo J, et al. The endosomal-lysosomal pathway is dysregulated by APOE4 expression *in vivo*. *Front Neurosci* 2017; 11: 702.
- Olofsson JK, Nordin S, Wiens S, Hedner M, Nilsson LG, Larsson M. Odor identification impairment in carriers of ApoE-varepsilon4 is independent of clinical dementia. *Neurobiol Aging* 2010; 31: 567–77.
- Ostrowski M, Carmo NB, Krumeich S, Fanget I, Raposo G, Savina A, et al. Rab27a and Rab27b control different steps of the exosome secretion pathway. *Nat Cell Biol* 2010; 12: 19–30; sup 1–13.
- Peng KY, Mathews PM, Levy E, Wilson DA. Apolipoprotein E4 causes early olfactory network abnormalities and short-term olfactory memory impairments. *Neuroscience* 2017; 343: 364–71.
- Perez-Gonzalez R, Gauthier SA, Kumar A, Levy E. The exosome secretory pathway transports amyloid precursor protein carboxyl-terminal fragments from the cell into the brain extracellular space. *J Biol Chem* 2012; 287: 43108–15.
- Pérez-González R, Gauthier SA, Kumar A, Saito M, Saito M, Levy E. A method for isolation of extracellular vesicles and characterization of exosomes from brain extracellular space. In: Hill AF, editor. *Exosomes and microvesicles: methods and protocols*. New York, NY: Springer; 2017. p. 139–51.
- Pfrefriger FW. Role of cholesterol in synapse formation and function. *Biochim Biophys Acta* 2003; 1610: 271–80.
- Raiborg C, Stenmark H. The ESCRT machinery in endosomal sorting of ubiquitylated membrane proteins. *Nature* 2009; 458: 445–52.
- Rajendran L, Bali J, Barr MM, Court FA, Kramer-Albers EM, Picou F, et al. Emerging roles of extracellular vesicles in the nervous system. *J Neurosci* 2014; 34: 15482–9.
- Razi M, Futter CE. Distinct roles for Tsg101 and Hrs in multivesicular body formation and inward vesiculation. *Mol Biol Cell* 2006; 17: 3469–83.
- Saito M, Wu G, Hui M, Masiello K, Dobrenis K, Ledeen RW, et al. Ganglioside accumulation in activated glia in the developing brain: comparison between WT and GalNAcT KO mice. *J Lipid Res* 2015; 56: 1434–48.
- Schreij AM, Fon EA, McPherson PS. Endocytic membrane trafficking and neurodegenerative disease. *Cell Mol Life Sci* 2016; 73: 1529–45.
- Sheline YI, Morris JC, Snyder AZ, Price JL, Yan Z, D'Angelo G, et al. APOE4 allele disrupts resting state fMRI connectivity in the absence of amyloid plaques or decreased CSF A β 42. *J Neurosci* 2010; 30: 17035–40.
- Shi J, Han P, Kuniyoshi SM. Cognitive impairment in neurological diseases: lessons from apolipoprotein E. *J Alzheimers Dis* 2014; 38: 1–9.
- Sing CF, Davignon J. Role of the apolipoprotein E polymorphism in determining normal plasma lipid and lipoprotein variation. *Am J Hum Genet* 1985; 37: 268–85.
- Strauss K, Goebel C, Runz H, Mobius W, Weiss S, Feussner I, et al. Exosome secretion ameliorates lysosomal storage of cholesterol in Niemann-Pick type C disease. *J Biol Chem* 2010; 285: 26279–88.
- Sullivan PM, Mezdour H, Aratani Y, Knouff C, Najib J, Reddick RL, et al. Targeted replacement of the mouse apolipoprotein E gene

- with the common human APOE3 allele enhances diet-induced hypercholesterolemia and atherosclerosis. *J Biol Chem* 1997; 272: 17972–80.
- Tai LM, Youmans KL, Jungbauer L, Yu C, Ladu MJ. Introducing human APOE into abeta transgenic mouse models. *Int J Alzheimers Dis* 2011; 2011: 810981.
- Tong LM, Yoon SY, Andrews-Zwilling Y, Yang A, Lin V, Lei H, et al. Enhancing GABA signaling during middle adulthood prevents age-dependent GABAergic interneuron decline and learning and memory deficits in ApoE4 mice. *J Neurosci* 2016; 36: 2316–22.
- Wisdom NM, Callahan JL, Hawkins KA. The effects of apolipoprotein E on non-impaired cognitive functioning: a meta-analysis. *Neurobiol Aging* 2011; 32: 63–74.
- Zhao N, Liu CC, Van Ingelgom AJ, Martens YA, Linares C, Knight JA, et al. Apolipoprotein E4 impairs neuronal insulin signaling by trapping insulin receptor in the endosomes. *Neuron* 2017; 96: 115–29.e5.